# An Ultrastable and Dense Single-Molecule Click Platform for Sensing Protein–Deoxyribonucleic Acid Interactions

small methods
www.small-methods.com

# An Ultrastable and Dense Single-Molecule Click Platform for Sensing Protein–Deoxyribonucleic Acid Interactions

*Emiel W. A. Visser,* Jovana Miladinovic, and Joshua N. Milstein**

**An ultrastable, highly dense single-molecule assay ideal for observing protein–DNA interactions is demonstrated. Stable click tethered particle motion leverages next generation click-chemistry to achieve an ultrahigh density of surface tethered reporter particles, and has low non-specific interactions, is stable at elevated temperatures to at least 45 °C, and is compatible with $Mg^{2+}$, an important ionic component of many regulatory protein–DNA interactions. Prepared samples remain stable, with little degradation, for >6 months in physiological buffers. These improvements enable the authors to study previously inaccessible sequence and temperature-dependent effects on DNA binding by the bacterial protein, histone-like nucleoid-structuring protein, a global transcriptional regulator found in *Escherichia coli*. This greatly improved assay can directly be translated to accelerate existing tethered particle-based, single-molecule biosensing applications.**

## 1. Introduction

Dynamic interactions between proteins and DNA are fundamental to the function and regulation of many cellular processes, ranging from DNA organization and gene transcription, to DNA replication and repair.[1] A versatile single-molecule technique for studying protein–DNA interactions is tethered particle motion (TPM) in which a reporter particle is bound to a substrate by a DNA tether.[2,3] The Brownian motion of the reporter particle is tracked under a microscope while the proteins in solution interact with the DNA.[4,5] The Brownian motion reflects changes in the flexibility or conformation (e.g., straightening, looping or kinking) of the DNA tether. Utilizing TPM, protein–DNA interaction,[6,7] transcription,[3,8] and DNA looping[9,10] have been successfully studied in vitro. Furthermore, significant effort has gone into developing TPM-derived sensing techniques to monitor the presence and concentration of medically relevant molecules over extended periods of time, making TPM a promising new method for biosensing applications. Recently, picomolar concentrations of nucleic acids were able to be continuously monitored, over several hours, in blood plasma by biosensing based on particle mobility,[11–13] while fM detection sensitivity to nucleic acids in bodily fluid samples was demonstrated by single-molecule tethering.[14]

The traditional TPM system has a few shortcomings that limit its applicability. The first is that the coupling strategy relies on both a streptavidin–biotin interaction and a much weaker antibody–antigen interaction. The antibody reliant coupling has a limited lifetime (typically a few hours), severely restricting the duration and conditions under which experiments can be performed. Second, it proves difficult in practice to achieve a high particle density due to denaturation and random orientation of surface absorbed antibodies. Additionally, the random orientation of the antibodies on the surface adds a variable length up to 15 nm to the tether.

Here, we demonstrate a significantly improved TPM assay that we dubbed stable click tethered particle motion (scTPM). In scTPM, the traditional antibody coupling strategy is replaced with trans-cyclooctene (TCO)–tetrazine bio-orthogonal click-chemistry at the surface as illustrated in **Figure 1**a.[15] The result is a strong covalent bond, which we find to be stable for months, and thus unlikely to break within the timeframe of a typical experiment or at higher, physiologically relevant temperatures. The TCO-activated surface is suitable for the attachment of other molecules of interest, and when combined with streptavidin-coated maleimide particles passivated with covalently linked bovine serum albumin (BSA), displays low non-specific interactions, creating a flexible platform for molecular TPM studies or biosensing applications.

The scTPM system was applied to probe sequence-dependent DNA interactions with the histone-like nucleoid-structuring protein (H-NS), a highly abundant regulatory protein found in proteobacteria such as *Escherichia coli* and *Salmonella*.[16–18] H-NS acts as a global transcriptional regulator and is key to the silencing of many horizontally acquired, xenogeneic genes associated with virulence and drug resistance.[16,19] Unlike traditional transcription factors, instead of binding strongly at a certain regulatory

Dr. E. W. A. Visser, J. Miladinovic, Prof. J. N. Milstein
Department of Chemical and Physical Sciences
University of Toronto Mississauga
Mississauga ON L5L 1C6, Canada
E-mail: e.w.a.visser@tue.nl; josh.milstein@utoronto.ca
Dr. E. W. A. Visser
Eindhoven University of Technology
Eindhoven 5612 AZ, The Netherlands
Prof. J. N. Milstein
Department of Physics
University of Toronto
Toronto ON M5S 1A1, Canada
The ORCID identification number(s) for the author(s) of this article can be found under https://doi.org/10.1002/smtd.202001180.



**DOI: 10.1002/smtd.202001180**

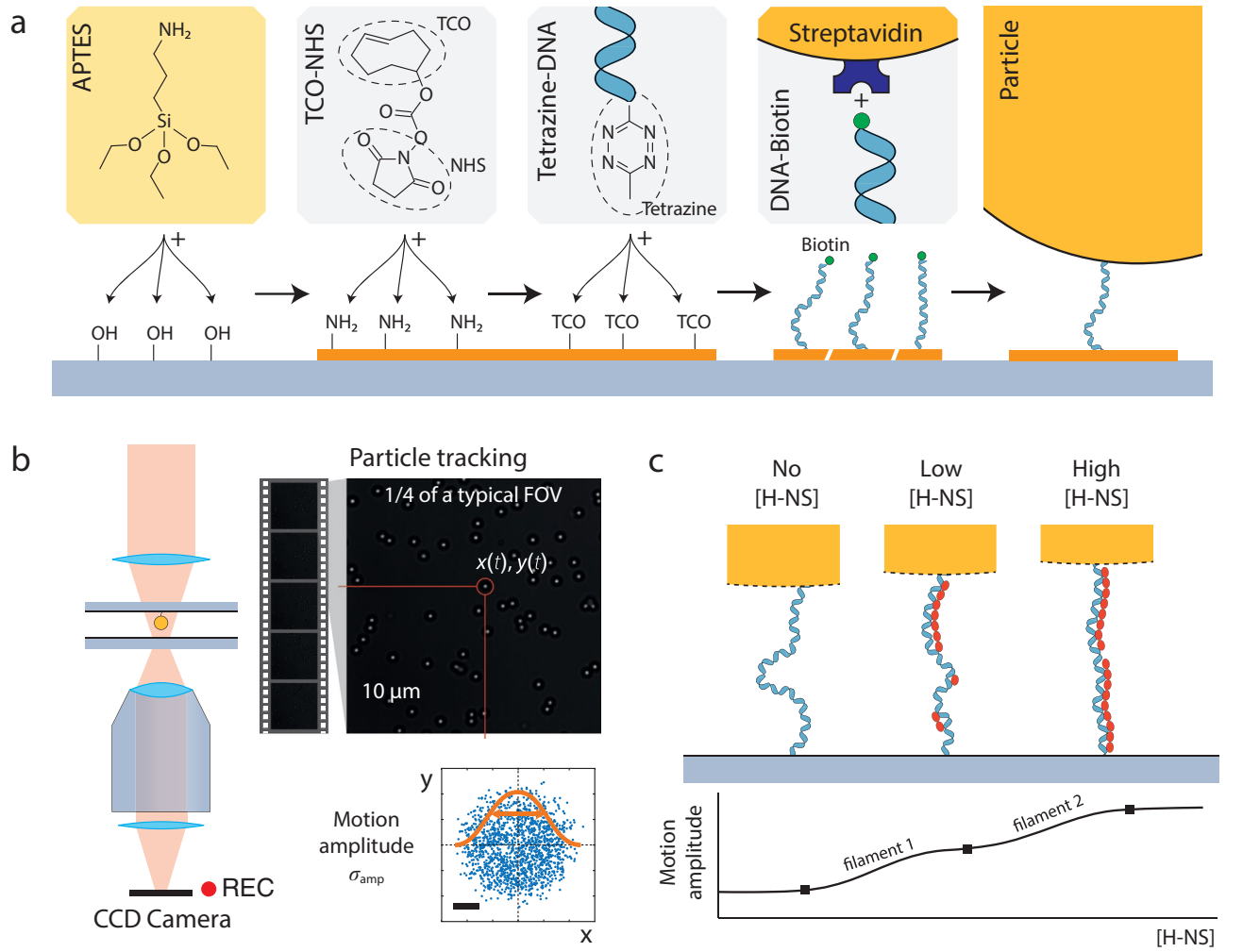


**Figure 1.** Illustration of the high-stability TPM implementation. a) Preparation steps of the surface to tether particles using the TCO–tetrazine click-chemistry. Left-to-right: APTES functionalization of bare glass, attachment of TCO groups using TCO-NHS, surface attachment of tethers using biotin- and tetrazine-labeled DNA, and attachment of streptavidin-labeled particles to biotin ligands on the DNA. b) Microscopy setup: the particle motion is recorded using a CCD camera on a brightfield microscope. Video data is analyzed and the motion pattern of the particles is determined. c) Illustration of the effect of [H-NS] on the motion amplitude. H-NS binds to DNA and forms filaments in the stiffening mode, increasing the end-to-end distance of the tether. Analysis of the motion amplitude as function of [H-NS] reveals the equilibrium dynamics of the filamentation.

sequence, H-NS is thought to loosely associate to AT-rich DNA where it may cooperatively form extended oligomeric filaments (although certain higher affinity sequences are also thought to act as nucleation sites for filament formation). This interaction between H-NS and DNA has been studied using ChIP,[16] optical and magnetic tweezers,[20–22] AFM,[23] and EMSAs.[24] As H-NS polymerizes along the DNA, it has been observed to stiffen it in the process, but can also compact the DNA by creating bridges between distant points on the DNA in the presence of $Mg^{2+}$.[1,19,22,23,25] While H-NS is well studied at both the genomic and ensemble level, the biophysical mechanism it actually employs to regulate gene expression remains controversial.[19]

The extreme stability and high density of scTPM enabled us to acquire the statistics needed to reveal sequence dependent effects on the binding of H-NS to promoter length DNA sequences (see Figure 1c). We performed protein concentration series to assess mechanical stiffening of the DNA through H-NS binding, for different trial sequences and at elevated temperatures inaccessible to traditional TPM assays.

## 2. Results and Discussion

scTPM samples were prepared as shown in Figure 1. A detailed description of the preparation method is given in the Experimental Section. We first verified the tethering quality of scTPM by studying the behavior of the tethered particles as a function of the DNA concentration (a proxy for DNA surface density). The particle motion was analyzed, and selection criteria were set to distinguish between single, multiple tethered, and stuck particles (see Figure S2, Supporting Information).[26] At [DNA] = 0 where particles can only be non-specifically bound to the surface, we typically find about 3 particles (range 0–20 particles) per field-of-view. Increasing the DNA surface density leads to an increase in bound particles, with a maximum of single bound particles at 2 pM (118 ± 12 particles per 84.5 × 84.5 µm$^2$. This optimum is followed by a decrease in single bound particles and an increase in multiple bound particles and finally to the formation of particles completely stuck through DNA binding. This confirms the full functionality of the scTPM

system. We routinely achieve a density of ≈4.2 particles per 100 μm$^2$, which approaches the theoretical maximum density of 20 particles per 100 μm$^2$ (see Supporting Information for details). Imaged on a microscope system with a 10× instead of a 60× objective, we managed to record 5084 properly tethered particles in a single field-of-view (see Figure S6, Supporting Information) demonstrating the scalability and high-throughput character of the scTPM assay.

Next, we generated a library of different DNA tether lengths which we incorporated into the scTPM system. The resulting motion amplitudes are shown in Figures S3 and S4 and Table S1, Supporting Information, for the scTPM coupling strategy and compared them to the simulation results[26] and the analytical model described by Segall et al.[27] An excellent match between experimental and simulation results is found, indicating the proper functionality of the generated tethers and the scTPM system.

Control experiments have been performed using freely diffusing particles in buffer containing up to 5 pM of $MgCl_2$ and up to 10 μm H-NS to determine non-specific binding. We typically observed less than five particles bound per field-of-view (84.5 × 84.5 μm$^2$). The stability of the improved TPM system was assessed through extended observation. Three samples were prepared with particles tethered to the surface, closed with tape, stored in the fridge, and measured for a period of up to 180 days. Some of the samples stored after other experiments were observed to fail through mechanisms unrelated to the scTPM system (some samples developed a bacterial infection and a few samples dried by evaporation of the buffer through the semipermeable tape used to cover some of the holes). The working samples demonstrate remarkable stability where the number of particles and the observed binding types remained the same after 180 days, as illustrated in Figure S5, Supporting Information, indicating that long term experiments can be performed with the scTPM system.

To demonstrate the utility of the scTPM system in biophysical applications, we applied it to study sequence dependent interactions between short, promoter length DNA sequences and H-NS. The influence of sequence on DNA binding by H-NS has proven difficult to be studied by single-molecule techniques and limited results have been published.[21,28]

Our results are shown in **Figure 2**. We consider H-NS binding with a synthetic 50% GC control strand with no strong nucleation site in absence of $Mg^{2+}$. With increasing [H-NS] the motion amplitude increases, indicating that H-NS binds to DNA in the filamentous, stiffening mode.[25] The observed amplitude change corresponds to the change in persistence length from 50 to 110 nm expected for DNA fully associated with H-NS.[22] Maximum stiffness is observed at 1 μM H-NS (measurements at higher concentrations do not show further stiffening, not shown). H-NS is present in *E. coli* at a copy number >2 × 10$^4$, which corresponds to a concentration on the order of 10 μM. A significant fraction of H-NS will be DNA-bound potentially lowering the free concentration of H-NS to below 1 μM. A structured interaction pattern is observed with three rising flanks and two plateau regions ≈20 and 200 nM H-NS, indicating that a complex interaction between DNA and H-NS exists even without the presence of a strong nucleation site. We hypothesize that this indicates the existence of three

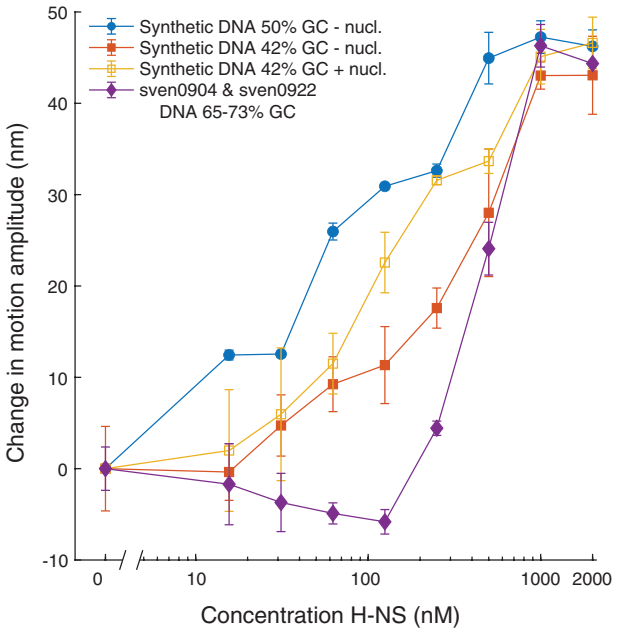


**Figure 2.** Change in (major) motion amplitude $A_{major}$ observed as function of the H-NS concentration for four different DNA tether sequences: 50% GC-content with no strong nucleation site (blue circles); 42% GC-content with (open yellow squares) and without (closed red squares) a Pribnow box nucleation site; and natural gene sections sven0904 and 0926 (purple diamonds). Data points represent the average of multiple measurement series (42%: three series each, 50%: two series, and sven0904 and sven0922: two series), error bars indicate the standard deviation of those values. All curves have been offset such that they converge for [H-NS] = 0 nM.

separate filamentation events in which distinct segments of the DNA become covered at different [H-NS]. It is likely that low- and high-affinity regions, as well as nucleation sequences, dictate the concentration dependent patterning of filaments along the DNA. At increasing [H-NS], two expanding filaments could continue to grow along vacant portions of the DNA until they eventually collide. At that [H-NS], further growth by the pair of filaments, at the two ends involved in the collision, would halt, an effect that could result in a plateauing of the stiffness.

Next, we study the effect of GC-content by comparing the 50% GC DNA to AT-rich DNA (42% GC—also no nucleation site). The interaction curve shifts to higher concentrations and the plateaus apparent in the 50% GC DNA construct are no longer apparent, with perhaps just one weaker plateau observed around [H-NS] = 100 nM. The apparent lower affinity is in contrast with the literature where, in general, a stronger affinity is observed between H-NS and AT-rich DNA. This general trend does not hold for all sequences and significant overlap in the observed binding of H-NS to DNA at low and neutral GC-content is observed in ChIP experiments.[16] The interaction curves indicate that sequence specific behavior has a profound effect on H-NS binding.

The effect of a nucleation site was assessed by repeating the experiment with the same 42% GC-content synthetic DNA, but with the bacterial promoter Pribnow box sequence TATAAT inserted at the center, a sequence known to strongly interact

with H-NS.[28] While the initial increase in the motion amplitude with [H-NS] remains relatively unaffected, the flank of the curve shifts to a lower [H-NS] of 100 nM, which is where the plateau was observed in the original sequence (absent the high-affinity insert). This observation is congruent with the expected stronger interaction between H-NS and the nucleation site and indicates that the central stepwise increase is likely related to the high-affinity sequence.

Then we consider the interaction between H-NS and segments of the promoter region of the genes 0904 (sven0904) and 0922 (sven0922) found in *Streptomyces Venezuelae* (65–73% GC-content).[29] Genes of *S. Venezuelae* are regulated by the H-NS analog Lsr2. Because Lsr2 and H-NS show a remarkable overlap in their interaction with DNA, the interaction of these gene fragments and H-NS is of interest.[28] The interaction curve in Figure 2 shows an initial slight decrease and subsequent strong rising flank. The shift to higher [H-NS] of the interaction curve agrees with the known lower affinity of H-NS for higher GC-content DNA. We hypothesize that the initial drop may be caused by H-NS inserting, perhaps into TA-steps, in the DNA and using its AT-hook to exacerbate the natural bend in AT sequences.[30] At higher [H-NS], filament formation takes over and stiffening is observed again. To the best of our knowledge such structured, concentration dependent interactions as we report here between DNA and H-NS have not been observed before. We hope to test our hypotheses and thus clarify the mechanism behind these novel observations in a future publication.

Finally, we demonstrate the extended application of the scTPM system by studying H-NS at elevated, biologically relevant temperatures. H-NS has previously been implicated in temperature sensing.[31] In addition to the usual reduced binding affinity at higher temperatures, H-NS has a thermosensitive switch that blocks DNA binding at elevated temperatures, affecting the regulation of gene expression (e.g., as bacteria transfer from ambient environments to the temperatures inside the human body).[31]

As a control we observe the effect of temperature on the sven0926 DNA tether (63.1% high GC-content) with temperatures increasing from 22 to 45 °C in **Figure 3**. The control melting curve (H-NS$^-$) shows that temperature has no significant effect on the observed motion amplitude. This matches our expectations. In the worm-like-chain description of dsDNA as a flexible polymer the temperature effects on the persistence length of dsDNA[32] cancel out with the Boltzmann factor. As the temperature has no effect on the observed amplitude, we thus conclude that an observed change in the motion amplitude is likely due to a change in the H-NS filament along the DNA.

We then observed the effect of temperature on DNA interacting with [H-NS] = 1 μM at temperatures increasing from room temperature to 38 °C (1 °C above gut temperature) in steps of 1.5 °C. The time between measurements was ≈15 min to allow for temperature equilibration on the setup. The measurements show a decreasing amplitude with increasing temperature, indicating a loss of DNA stiffening by H-NS. This effect could result either from H-NS unbinding from the DNA or from a change in the interaction of H-NS with the DNA and/or neighboring H-NS molecules. The curve shows a gradual decrease in the motion amplitude with the steepest decrease occurring between 26 and 27 °C. At 38 °C, the curve approaches the bare DNA (H-NS$^-$) curve, indicating that only some of the stiffening effect remains. An autoinhibitory temperature switch in H-NS is known to block self-association at elevated temperatures.[31] Our results indicate that the temperature switch has a continuous response over the entire range of 22–38 °C.

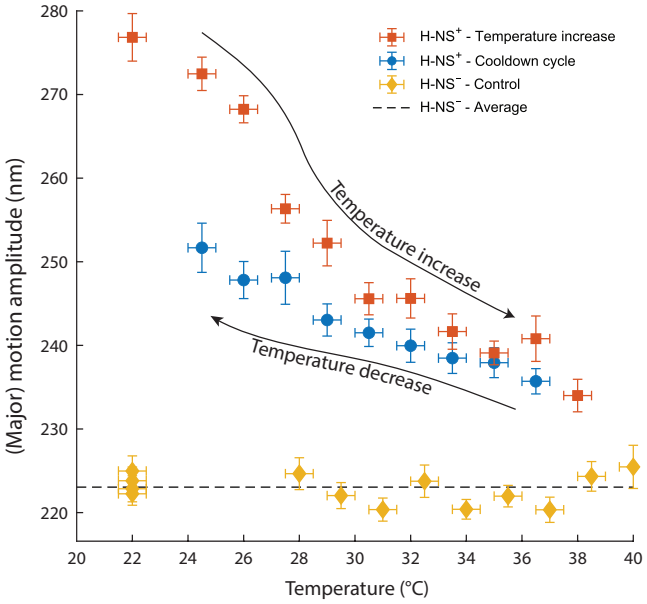


**Figure 3.** Effect of temperature on the amplitude of motion of 3.5 pM sven0926-tethered particles in the absence of H-NS (H-NS$^-$) and in presence of 1 μM H-NS (H-NS$^+$). The curves with temperatures increasing and decreasing are shown separately. Horizontal error bars indicate the 0.5 °C uncertainty in the temperature and vertical error bars indicate the standard error of the mean of the observed motion amplitude.

After the temperature increases, the temperature was decreased to 24 °C in steps of 1.5 °C and the particle motion was recorded at each stop. A partial recovery of the motion amplitude was observed. A full recovery was not observed likely because of denaturation of H-NS over the ≈4.5-h measurement period. The recovery indicates that the effect is, at least, partly due to a reversible change, as expected for a molecular temperature switch.

## 3. Conclusion

We have demonstrated a greatly improved, highly stabile TPM system (scTPM) to study interactions between proteins and DNA. Where traditional TPM relies on weak antibody coupling, which dissociates more rapidly at increasing temperatures and adds between 0 and 15 nm of variability to the tether length due to its orientation, the scTPM systems creates strongly bound particles with a well-controlled tether length with no length variation. The ultrastable click-chemistry of scTPM enables long-term studies, far exceeding the few hours obtainable with traditional TPM (measurement ready samples can remain stable for 6 months or longer), and measurements at elevated temperatures up to at least 45 °C. As far as we are aware, such a long-lived TPM system has not been reported before in the

literature. The high reporter particle densities we demonstrate ensure massively parallel experimentation. With a density of ≈4.2 particles per 100 $\mu m^2$, scTPM is on par with a high-throughput TPM assay leveraging surface micropatterning (requiring more complicated microfabrication) to optimize the particle-density to ≈2.7 particles per 100 $\mu m^2$.[33] By combining micropatterning and covalent click-chemistry we would be able to approach the theoretical limit of ≈20 particles per 100 $\mu m^2$ for a system with 1 µm particles tethered with 1 kb DNA.

These improvements enabled us to study previously inaccessible sequence and temperature-dependent effects on the interaction between H-NS and DNA. We find that H-NS interacts with DNA sequences in a highly structured manner, with H-NS filaments likely forming in stages with increasing [H-NS]. The introduction of a 6 bp H-NS nucleation site in the sequence was observed to significantly lower the concentration at which the filament starts to form. Likewise, H-NS filaments along the DNA were observed to soften at increasing temperatures, while regaining their original stiffness upon cooling, hinting at a biophysical mechanism behind H-NS's role as a temperature dependent molecular switch. These results illustrate the sensitivity of scTPM for finely probing novel protein–DNA interactions.

The scTPM system would clearly enhance current single-molecule force spectroscopy methods such as magnetic or optical tweezers. However, we foresee a range of applications for scTPM well beyond biophysical research. For medical applications, single-molecule biomarker monitoring and detection methods based on TPM have been demonstrated previously.[11–14] The high-stability and low non-specific interactions of the scTPM platform can be used to produce biomarker detection sensors that remain functional for weeks to months at a time and under a range of environmental conditions. The TCO click sensing surface forms a flexible platform for the attachment of nucleotides, proteins, and enzymes, and the scTPM surface can be readily functionalized with the required ligands for biomarker capture or the biomarker analog for a competition assay. The click-ready surface enables spatial multiplexing measurements using micropatterning techniques such as microcontact printing or microspotting to generate spatially multiplexed sensor surfaces. Different detection ligands in discrete locations would form a spatially multiplexed sensor akin to a DNA microarray plate in which multiple biomarkers can be simultaneously detected. These properties make scTPM an excellent platform for the creation of medical biomarker sensors. Such sensors require long term stability of the sensing platform and low backgrounds, both of which can be provided by scTPM. Incorporated into a TPM-based medical sensor, scTPM would enable one to follow the state of patients in critical conditions by reliably monitoring molecular biomarkers, for up to several months, improving the chance of a positive outcome for these cases. We foresee that scTPM will be applied both as a research tool and a medical technology.

## 4. Experimental Section

*Surface Functionalization*: Glass cover slips were plasma-cleaned for 15 min and APTES (99%, Sigma Aldrich, 440140)-functionalized for 1 h in 1 v/v% APTES in anhydrous toluene. Slides were then thoroughly bathed and rinsed in sequence with methanol, ethanol, and twice MilliQ water to wash the slides. Slides were dried using a stream of clean compressed air and then baked overnight at 110 °C to crosslink the APTES layer. Slides were stored in a vacuum chamber until further use.

*Flow Chamber Assembly*: Ten fluid access ports were drilled in glass cover slides using diamond powder coated drill bits. Flow chambers were cut from 300LSE double-sided adhesive film (3M, Saint Paul, USA) using a plotter cutter (CM350e, Brother). The double-sided adhesive was used to attach the APTES-functionalized glass to the microscope slides, forming five parallel reaction chambers with two fluid access ports each.

*Particle Functionalization*: Carboxylic functionalized melamine particles (MF-COOH-AR586, microParticles GmbH, Berlin, Germany) were functionalized with Streptavidin (Sigma Aldrich, 85878) and BSA using an EDC (Sigma Aldrich, E6383) coupling strategy. Each time particles were washed or a buffer exchange was required the particles were centrifuged for 30 s at 10.000 × *g* centrifugation and the supernatant was removed using a pipette. Particles were incubated for 1 h in NaOH (0.01 M) and washed trice with MES buffer (25 mM, pH 4.5). The washed particles were activated in a solution of EDC (10 mg) in anhydrous DMSO (150 µL, ≥99.9%, 276855, Sigma Aldrich) and cold MilliQ (400 µL) on a tube rotator in the fridge. The particles were then washed with cold MilliQ water, sonicated for 10 s and washed with cold MES buffer. Next, they were resuspended in PBS (50 µL) containing Streptavidin (0.5 µg $mL^{-1}$) for 5 min and then mixed with PBS (950 µL) containing BSA (10 mg $mL^{-1}$) and incubated overnight on a tube rotator in the fridge. Particles were then washed twice with MES buffer (200 µL) with a 30 s-sonication in a sonic bath to break up particle clusters. Finally, the particles were resuspended in filter sterilized storage buffer PBS with BSA (1 mg $ml^{-1}$), Tween-20 (0.05 v/v%).

*Deoxyribonucleic Acid Strand Assembly*: DNA sequences (linear gBlock Gene Fragments), ssDNA sequences, primers, and biotin/azide-labeled primers were obtained from IDT (Coralville, IA, USA). The tetrazine-labeled primer was prepared by reacting the azide-labeled primer 1:1 with methyltetrazine-DBCO (Click Chemistry Tools, Scottsdale, AZ, USA). PCR results were verified on a 1.5% agarose TAE gel, products were cleaned up using PCR cleanup kits (EZ-10 PCR Product Purification Kit, Bio-basic, Amherst, NY, USA), and concentrations were measured on a spectrophotometer (Implen Nanophotometer P330). DNA products were stored at −20 °C in TE buffer. The method is illustrated in Figure S1, Supporting Information.

*Synthetic DNA*: The synthetic template DNA was circularized using an ssDNA segment with 18–23 nt overlap at both ends (sequences in Supporting Information) in a Gibson assembly reaction using HiFi DNA Assembly Master Mix from New England Biolabs (Ipswich, MA, USA) to generate the template for the next step. The inserted sequence was determined by the ssDNA sequence. The generated template was directly amplified using the biotin- and tetrazine-labeled primers as the primer binding locations were built into the designed sequence.

*DNA from Natural Templates*: Two consecutive PCR reactions were performed for DNA templates of natural source. The first PCR amplified the section of interest from the natural template using primers with overhangs to generate the template for the second PCR. The second PCR was then performed with the biotin- and the tetrazine-labeled primers that attach to the earlier formed overhangs forming the final product with the appropriate labels.

*Stable Click Tethered Particle Motion System Integration*: TCO-PEG4-NHS (Click Chemistry Tools, Scottsdale, AZ, USA) was incubated at a concentration of 1 mM in PBS containing 10 v/v% DMSO (anhydrous, ≥99.9%, 276855, Sigma Aldrich) in the assembled flow chamber for 1 h at room temperature. Chambers were then flushed with MilliQ water (100 µL), dried using clean air or nitrogen, and flushed with PBS (100 µL). DNA tethers were incubated at the required concentration (typically 3.5 pM) for 90 min. The chambers were flushed twice with PBS (100 µL). Functionalized particles were then flown into the chamber from stock solution at a 15:100 dilution with BSA solution (10 mg $mL^{-1}$ BSA in PBS) and incubated for at least 30 min. Optionally the chambers were inverted and flushed using the BSA solution to flush out unbound particles.

*Measurements*: H-NS proteins were diluted into HKE reaction buffer (25 mM HEPES, 50 mM KCl, and 0.1 mM EDTA) and flown into the chambers through the fluid ports. Measurements were taken on a home-build microscope using a Nikon 60× Plan Apo objective (Tokyo, Japan) using brightfield illumination and an Andor iXon Ultra 897 emCCD camera. Typical camera settings: 5 ms exposure time, full frame: 512 × 512 pixels, 25 frames/s, and no EM gain. Pixel size calibration (165.5 nm/pixel) was performed through imaging a square grid with known spacing. The data was analyzed using analysis code written in MATLAB described in earlier work.[11]

## Supporting Information

Supporting Information is available from the Wiley Online Library or from the author.

## Acknowledgements

The authors thank Paul Piunno for his helpful discussions on optimizing the APTES functionalization, William Navarre for providing the H-NS proteins, and Marie Elliot and Xiafei Zhang for providing the natural DNA templates from *Streptomyces venezuelae*. This project has received funding from the European Union's Horizon 2020 research and innovation programme under grant agreement No. 796345, and from a National Sciences and Engineering Research Council of Canada Discovery Grant (RGPIN-2019-06520).

## Conflict of Interest

The authors declare no conflict of interest.

## Author Contributions

E.W.A.V. and J.N.M. conceived and designed the methodology, measurement system, and experiments. E.W.A.V. and J.M. performed the experiments. E.W.A.V. performed the simulations. E.W.A.V., J.M., and J.N.M. interpreted the results and wrote the manuscript.

## Data Availability Statement

The data that support the findings of this study are available from the corresponding author upon reasonable request.

## Keywords

biomarker sensing platforms, click-chemistry, high-stability, histone-like nucleoid-structuring proteins, protein–deoxyribonucleic acid interactions, tethered particle motion

Received: November 26, 2020
Revised: January 29, 2021
Published online:

[1] D. Song, J. J. Loparo, *Trends Genet.* **2015**, *31*, 164.
[2] D. A. Schafer, J. Gelles, M. P. Sheetz, R. Landick, *Nature* **1991**, *352*, 444.
[3] H. Yin, R. Landick, J. Gelles, *Biophys. J.* **1994**, *67*, 2468.
[4] L. Finzi, J. Gelles, *Science* **1995**, *267*, 378.
[5] D. Dunlap, C. Zurla, C. Manzo, L. Finzi, in *Single Molecule Analysis*, (Eds: E. J. G. Peterman, G. J. L. Wuite), Humana Press, New York **2011**, pp. 295–313.
[6] H.-F. Fan, C.-H. Ma, M. Jayaram, *Micromachines* **2018**, *9*, 216.
[7] H.-F. Fan, C.-H. Ma, M. Jayaram, *Nucleic Acids Res.* **2013**, *41*, 7031.
[8] H. Yin, I. Artsimovitch, R. Landick, J. Gelles, *Proc. Natl. Acad. Sci. USA* **1999**, *96*, 13124.
[9] Y. Y. Biton, S. Kumar, D. Dunlap, D. Swigon, *PLoS One* **2014**, *9*, e92475.
[10] Y.-F. Chen, J. N. Milstein, J.-C. Meiners, *Phys. Rev. Lett.* **2010**, *104*, 258103.
[11] E. W. A. Visser, J. Yan, L. J. van IJzendoorn, M. W. J. Prins, *Nat. Commun.* **2018**, *9*, 2541.
[12] J. Yan, L. van Smeden, M. Merkx, P. Zijlstra, M. W. J. Prins, *ACS Sens.* **2020**, *5*, 1168.
[13] R. M. Lubken, A. M. de Jong, M. W. J. Prins, *Nano Lett.* **2020**, *20*, 2296.
[14] W.-C. Cheng, T. Horn, M. Zayats, G. Rizk, S. Major, H. Zhu, J. Russell, Z. Xu, R. E. Rothman, A. Celedon, *Nat. Commun.* **2020**, *11*, 4774.
[15] R. Selvaraj, J. M. Fox, *Curr. Opin. Chem. Biol.* **2013**, *17*, 753.
[16] W. W. Navarre, S. Porwollik, Y. Wang, M. McClelland, H. Rosen, S. J. Libby, F. C. Fang, *Science* **2006**, *313*, 236.
[17] D. C. Grainger, *Biochem. Soc. Trans.* **2016**, *44*, 1561.
[18] T. Atlung, H. Ingmer, *Mol. Microbiol.* **1997**, *24*, 7.
[19] K. Singh, J. N. Milstein, W. W. Navarre, *Annu. Rev. Microbiol.* **2016**, *70*, 199.
[20] R. S. Winardhi, J. Yan, L. J. Kenney, *Biophys. J.* **2015**, *109*, 1321.
[21] R. Gulvady, Y. Gao, L. J. Kenney, J. Yan, *Nucleic Acids Res.* **2018**, *46*, 10216.
[22] H. Wang, S. Yehoshua, S. S. Ali, W. W. Navarre, J. N. Milstein, *Nucleic Acids Res.* **2014**, *42*, 11921.
[23] R. T. Dame, C. Wyman, N. Goosen, *Nucleic Acids Res.* **2000**, *28*, 3504.
[24] C. C. Brescia, M. K. Kaw, D. D. Sledjeski, *J. Mol. Biol.* **2004**, *339*, 505.
[25] Y. Liu, H. Chen, L. J. Kenney, J. Yan, *Genes Dev.* **2010**, *24*, 339.
[26] E. W. A. Visser, L. J. van IJzendoorn, M. W. J. Prins, *ACS Nano* **2016**, *10*, 3093.
[27] D. E. Segall, P. C. Nelson, R. Phillips, *Phys. Rev. Lett.* **2006**, *96*, 088306.
[28] B. R. G. Gordon, Y. Li, A. Cote, M. T. Weirauch, P. Ding, T. R. Hughes, W. W. Navarre, B. Xia, J. Liu, *Proc. Natl. Acad. Sci. USA* **2011**, *108*, 10690.
[29] L. T. Fernández-Martínez, C. Borsetto, J. P. Gomez-Escribano, M. J. Bibb, M. M. Al-Bassam, G. Chandra, M. J. Bibb, *Antimicrob. Agents Chemother.* **2014**, *58*, 7441.
[30] R. A. van der Valk, J. Vreede, L. Qin, G. F. Moolenaar, A. Hofmann, N. Goosen, R. T. Dame, *eLife* **2017**, *6*, e27369.
[31] U. F. S. Hameed, C. Liao, A. K. Radhakrishnan, F. Huser, S. S. Aljedani, X. Zhao, A. A. Momin, F. A. Melo, X. Guo, C. Brooks, Y. Li, X. Cui, X. Gao, J. E. Ladbury, Ł. Jaremko, M. Jaremko, J. Li, S. T. Arold, *Nucleic Acids Res.* **2019**, *47*, 2666.
[32] S. Geggier, A. Kotlyar, A. Vologodskii, *Nucleic Acids Res.* **2011**, *39*, 1419.
[33] T. Plénat, C. Tardin, P. Rousseau, L. Salomé, *Nucleic Acids Res.* **2012**, *40*, e89.